



Polystyrene and Polymethylmethacrylate Microplastics Embedded in Fat, Oil, and Grease (FOG) Deposits of Sewers

Mitra Nikpay

Faculty of Civil Engineering, Dresden University of Applied Sciences, 01069, Dresden, Germany

Received: 03-05-2022, Revised: 16.06.2022, Accepted: 09.07.2022

Abstract

Fat, oil, and grease (FOG) deposits in the urban sewer system affect the optimal performance of the wastewater collection system and treatment plant, while increasing sewer maintenance costs. The interaction of microplastics (MPs) and FOG in the sewer system could drastically change the quality of deposited materials and the fate of MPs in raw sewage. In this study, the batch experiment was conducted to explain the mechanism of FOG formation by synthetic wastewater and its interaction with polystyrene (PS) and polymethyl methacrylate (PMMA) particles. We found three different segments for FOG deposits in the batch, namely static and buoyant micro-deposits, gel-like, and solid deposits. The average size of micro-deposits adhered to the solid-liquid interface of the container was 25 μm and buoyant deposits with a small size of 3 μm adsorbed onto the MPs at the liquid-air interface. The gel-like formation promoted a virtual liquid phase where PS and PMMA were confined and segregated. Some PMMA particles were entrapped in the self-assembly of biopolymers that formed between the PS particles. This research indicates that FOG deposition in the urban sewers contains high numbers of MPs, such that any plan involving a reuse or disposal program requires a risk assessment.

Keywords: Segregation, Biopolymer, Polystyrene, PMMA, Surfactant

INTRODUCTION

Microplastics (MPs) are emerging contaminants introduced into wastewater since the industrial manufacture of the synthetic polymer in the early 1950s while its production and anthropogenic impacts are increasing rapidly to date (Ainali et al., 2022; Viaroli et al., 2022; Azizi et al., 2022; Razeghi et al., 2021; Adib et al., 2021; Alavian Petroody et al., 2021; Schessl et al., 2019; Dehghani et al., 2017). Due to the enormous terrestrial impact of MPs, there is still a lack of qualitative/quantitative information on the aspects related to interfaces, especially between MPs and wastewater in the wastewater collection, treatment, and disposal systems. The interaction of MPs with fat, oil, and grease (FOG) in the urban sewers is a critical issue that requires in-depth study due to its importance for the operation and maintenance of sewer system (Nikpay, 2022).

Urban wastewater collection systems accumulate FOG from the household, food service, and industrial wastewater in the form of hardened solids which leads to sewer pipe blockages and eventually sewer overflows and implies financial losses (Wallace et al., 2017; He et al., 2013). Sewer overflow could disperse high concentrations of organic and inorganic constituents, including pathogens and MPs, into open spaces and pose a public health hazard. FOG in sewers is related to people's dietary habits and estimates at 50 kg/yr and 20 kg/yr for developed and less developed countries, respectively (Williams et al., 2012).

FOG deposits are formed by the saponification process of saturated fat with palmitic as

* Corresponding author Email: nikpay11@gmail.com

primary fatty acid and calcium (Ca^{+2}) as the primary metal (He et al., 2011; Keener et al., 2008). Two important sources of Ca^{+2} in wastewater are water hardness and corrosion of concrete pipes (He et al., 2013; Williams et al., 2012). Ca^{+2} in natural waters results from the dissolution of polyvalent metal ions by the passage of water between rocks and soil or by the seepage of pollutants. Ca^{+2} and magnesium (Mg^{+2}) are the main contributors to the hardness value, while other metals such as aluminum, barium, manganese, strontium, and zinc contribute only slightly (Sepehr et al., 2013). The concrete source of Ca^{+2} in wastewater resulted from the corrosion by the acidic form of H_2S at concentrations above 2 ppm, especially in the partially filled gravity pipes (Li et al., 2017). Microbial deterioration of concrete by anaerobic sulfate-reducing (SRB) and sulfur-oxidizing bacteria (SOB), starting with the production of hydrogen sulfide (H_2S), decreasing the concrete pH from 12 to 9, and finally the production of sulfuric acid (H_2SO_4) and the reduction of pH to ~ 1 (Huber et al., 2016; Bielefeldt et al., 2010; Roberts et al., 2002; Clark et al., 1999). The reaction of sulfuric acid with cement leads to the formation of gypsum ($\text{CaSO}_4 \cdot 2\text{H}_2\text{O}$) and later to form ettringite ($3\text{CaO} \cdot \text{Al}_2\text{O}_3 \cdot 3\text{CaSO}_4 \cdot 32\text{H}_2\text{O}$), which increases the calcium concentration of the wastewater (O'Connell et al., 2010, Satoh et al., 2010).

The initial FOG deposits in the form of micro-deposits adhere to the inner walls of the pipes or float at the liquid-air interfaces. Nieuwenhuis et al., (2018) measured the density of FOG in sewers about 1.0 g/cm^3 , which explains the floatability of the micro-deposits at the liquid-air interfaces. The small deposits gradually grow in size and allow other wastewater components, including MPs, to stick in their aggregation. The latter contributes to form more layers with high yield strength, eventually increasing the size of aggregated FOG-based materials (Otsuka et al., 2020; Keener et al. 2008). In addition, the release of various polar and nonpolar surfactants in sewers could separate the FOG from the liquid phase with different mechanisms such as emulsion, adsorption, foaming, or reverse micelles and make FOG deposits more susceptible to the adsorption of dispersed MPs (Bergfreund et al., 2021; Ingram et al., 2013).

The present study aims to investigate the interaction between MPs and FOG deposits using batch experiments and employ micro-size particles of polystyrene (PS) and polymethyl methacrylate (PMMA) in the synthetic wastewater. Visualization and image processing techniques were used to qualify and, as far as technically possible, to quantify the interaction between MPs and FOG deposits.

MATERIALS AND METHODS

Synthetic wastewater formulated according to the constituents listed in Table 1 to simulate the FOG formation process in the sewer. Stearic, palmitic, and oleic acids are various saturated and unsaturated fatty acids occurring naturally in plants and animals and widely used in industry, e.g., in the production of rubber, lubricants, dispersants, and plasticizers. The addition of palmitic and oleic acids, as well as Ca^{2+} , increases the FOG deposit yield strength of the wastewater (Gross et al., 2017). Surfactants comprise another group of wastewater constituents that enter the sewer system by the use of detergents from households or industries. Surfactants used in the synthetic wastewater solution are sodium dodecylbenzene sulfonate surfactant (SDBS), hexadecyltrimethyl-ammonium bromide (CTAB), and Triton X-100. Quartz represents inorganic fines that are part of the wastewater matrix and affect the adsorption behavior of pollutants into MPs surfaces (Nikpay, 2022). Iron oxide is one of the heavy metals that enter the sewer system by industrial activities, corrosion of pipes, roofs, and road runoff (Ida and Eva, 2021).

After addition of the constituents of Table 1 to the deionized water, the solution was placed in an ultrasonic device for 45 min and in a preheated oven at $70 \text{ }^\circ\text{C}$ for 5 min. The pH of the solution was measured at ~ 6.5 and the temperature at $\sim 20 \text{ }^\circ\text{C}$. The materials used for this experiment were purchased from Sigma Aldrich Co.

The particles used in the test are clean spherical polystyrene (PS) and polymethyl methacrylate

Table 1. Components of synthetic wastewater solution

Constituents	Purity %	Concentration mg/l
Stearic acid	98.5	33
Palmitic acid	99	34
Oleic acid	99	33
SDBS	99	7.5
CTAB	98	1.5
TX-100	95	10.2
Calcium chloride	97	74
Quartz <297 μm	-	273
Iron oxide II/ III<5 μm	95	1

(PMMA), purchased from Sigma Aldrich Co. The color of PS is red with an average size of 60 μm , and PMMA, also known as acrylic glass, is transparent white with a size of 900 μm . The density of PS is 1.05 g/cm^3 and for PMMA 1.18 g/cm^3 , with contact angles for water in air of 86° and 67°, respectively. This means that PS is rather hydrophobic and PMMA has hydrophilic characteristics (Verdú et al, 2022; Tokuda et al., 2015; Li et al., 2007; Howse et al., 2001). PS and PMMA have a wide range of applications in industry and households.

To simulate the condition of wastewater in the sewer system, a wide-mouth beaker was filled with 70 ml of synthetic wastewater and the experiment was repeated for three additional identical solutions. A quantity of 6.8 mg PS and 3.5 mg of PMMA were weighed using METTLER TOLEDO AT261 Delta Range analytical balance and added to the solution. After that, the beaker was covered with parafilm and placed on the IKA Vibrax VXR with orbital motion of 180 rpm for 168 hours. The solution containing the MPs was carefully transferred to another container to allow detection of the adsorbed FOG deposit at the bottom of beaker using the Müller GmbH stereomicroscope equipped with a digital camera DCM310. The MPs and solution also were examined under the microscope and the recorded images were analyzed using ImageJ software.

RESULTS AND DISCUSSION

Micro-deposits

FOG deposits in the batch were observed at the microscopic level and in large quantities. Two types of deposits were identified: the static form was deposited at the bottom of the beaker, and the buoyant form was located at the liquid-air interface of the solution.

Fig.1a shows dense white micro-deposits of FOG at the bottom of the glass container. The highlighted patch in the image explains the further steps of thresholding and the measured deposits in Fig.1a₁, a₂ using particle analyzing method (Igathinathane et al., 2008). Fig.1b shows the graph of the normal distribution of the counted micro-deposits to their diameter, where the micro-deposits with a size of 25 μm are dominant. Fig.1c displays the graph of cumulative area of FOG micro-deposits versus the number of their counts for Fig.1a with an image size of 3.01×2.26 mm. The linear fit model with a determination coefficient $R^2= 0.99$ expressed the equation for the measured area shown in the table of Fig.1c.

Fig.2a illustrates several discrete crystalline FOG micro-deposits that are buoyant at the liquid-air interfaces due to their low density, which is intensified by the addition of surfactants. A mixture of CTAB, SDS, and Triton X-100 participated in adsorption on the hydrophobic surfaces of the buoyant FOG micro-deposits and contributed to the adsorption of charged and uncharged molecules. As a result, the deposit was less prone to the adsorption of water molecules,

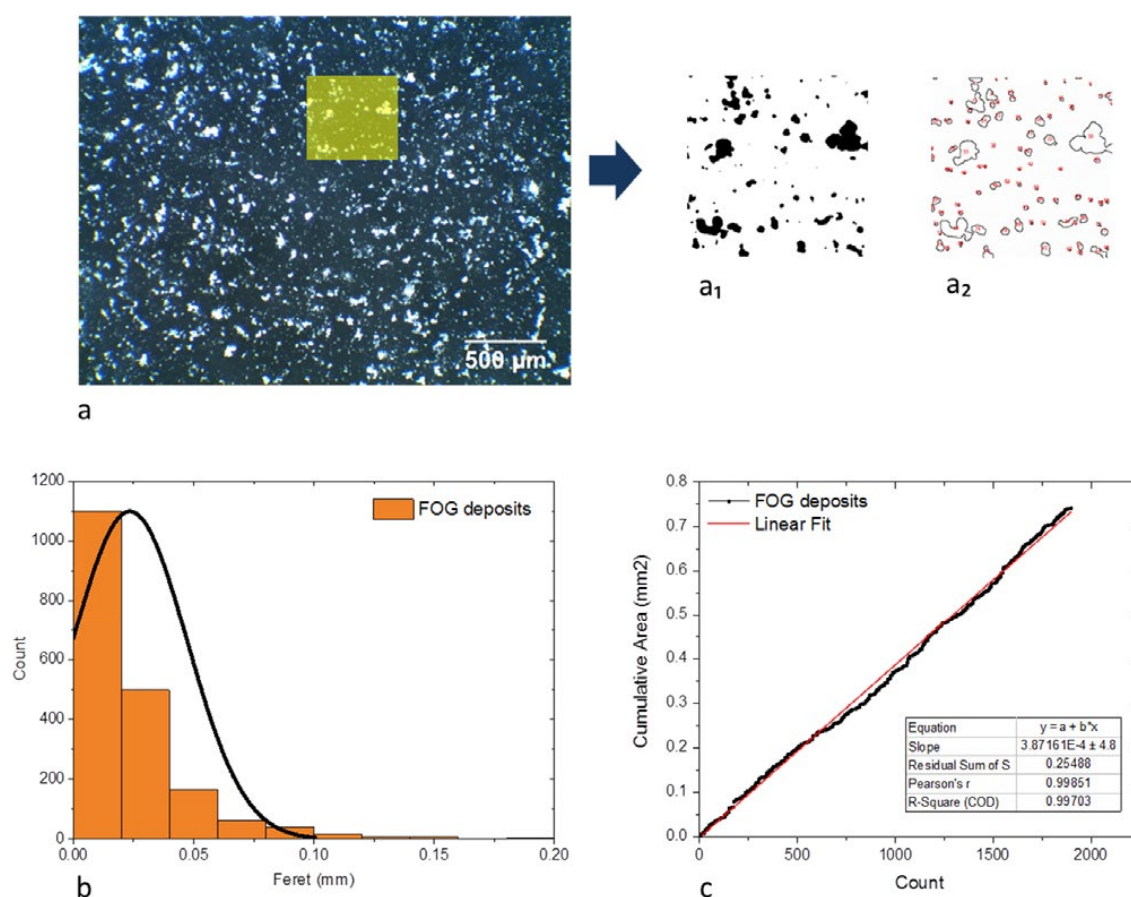


Fig. 1. a) The image of FOG micro-deposits detected at the bottom of the beaker. The highlighted patch is processed to count the deposits shown in a₁ and a₂. b) The graph of the normal distribution and c) cumulative area of the counted micro-deposits from the image (a).

which affected the density of the final deposit. Such a product adsorbs on the MPs surfaces and confines the MPs inside the sticky materials. Likewise, adsorption of surfactants on the MPs surfaces could actively change the surface charge properties. The hydrophilic PMMA particles enable the adsorption of charged CTAB molecules by electrostatic attraction, with the head towards the particle surfaces and the tail directed to bulk. The anionic SDS joins the interface by the head towards the surface, forming a paired SDS-CTAB charge on the PMMA surfaces. On the other hand, the PS exhibits a hydrophobic surface with no significant polar contribution to the surface energy. Since the electrostatic repulsion is low, the hydrophobic force overcomes the electrostatic attraction.

Fig.2b shows the adhesion of FOG micro-deposits with the size of less than 40 μm to the PMMA surfaces. Looking at Fig.2c, the aggregated micro-deposits become larger but are still buoyant and confining more microplastic (MP) particles. Some PS particles remained buoyant at the liquid-air interfaces of the synthetic wastewater, and the micro-deposits adsorbed onto their surfaces, which is apparent in Fig.2d. The adsorption mechanism between the PS and the micro-deposits resulted from the hydrophobic force of the PS. This force changes the three-phase contact angle of the air-liquid-solid interfaces due to the surface deformation of the liquid around the PS particle and the convective flow generated by the buoyant deposits.

The fatty acids crystals can generate convective flow at the liquid-air interface due to Marangoni and capillary effects (See Fig.2c, e), attributed to temperature variations or chemical

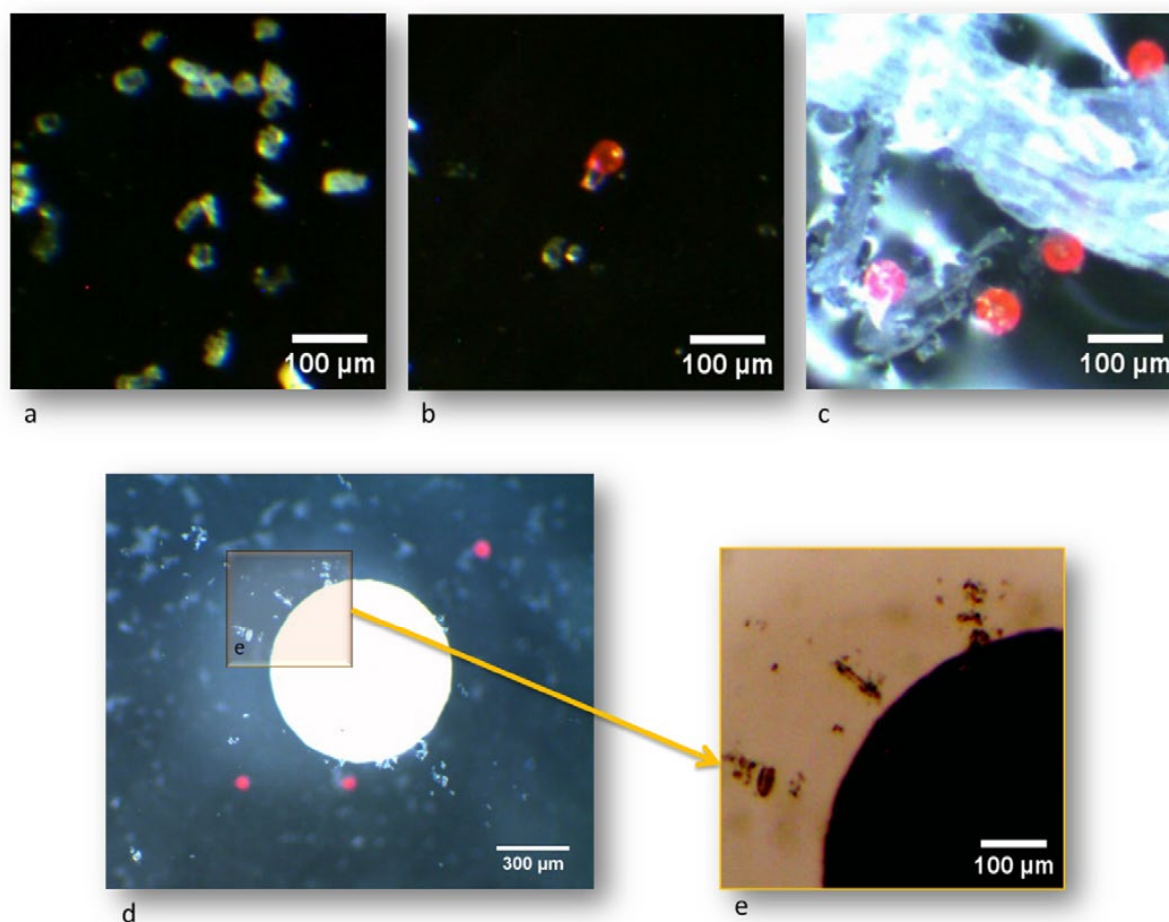


Fig. 2. a) The buoyant FOG deposits at the air-liquid interfaces, b) the adhesion of micro-deposits to the PMMA surfaces, and c) the aggregated buoyant deposits entrapping the PMMA particles. d) Alignment of the buoyant FOG deposits to the PS particle and e) detailed adsorption process for the selected part of (d).

compositions (Bansagi et al., 2013). The motion mechanism could also be influenced by the surfactant activity at the liquid-air interfaces. Eventually, complex surface flow occurs between the buoyant deposits and the MP, inducing deposit clusters that align with the MP surfaces (See Fig.2e).

Gel-like deposit

Part of the FOG deposit in the batch turned into a gel-like phase of transparent white color. Fig.3a, b shows a gel-like phase that separated from the rest of the solution where the PMMA and PS particles were confined. In general, the gel phase induces by double-bond fatty acid chains. The gel postulated a virtual phase within the wastewater solution and segregated a two-phase liquid-liquid system. Segregation was also observed in PS and PMMA particles due to differences in size, density, shape, or surface roughness of the particles, resulting in non-uniform distribution of the particles in bulk (Jain et al., 2013).

Fig.3 shows the segregation of the particles in the batch due to the passage of PMMA (~60 μm) through the voids between the PS particles (~900 μm). The latter is the outcome of the mechanical vibration or less motion of the PS particles, allowing the PMMA particles to

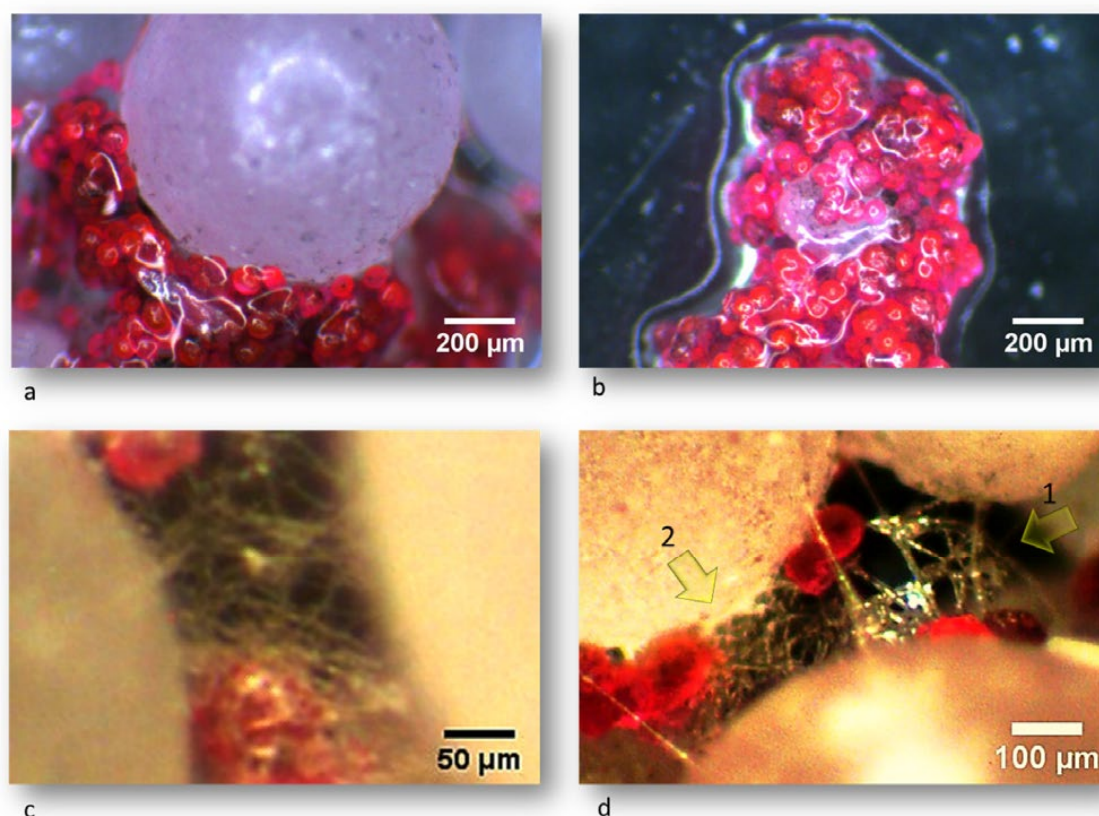


Fig. 3. a) A gel-like phase with confined MPs inside and b) segregated PMMA particles. c) Formation of biopolymers in voids between the PS and PMMA particles and d) the regular star shapes (1) and knitted parts (2).

percolate downward by gravity. The process will be more complex as it involves a viscous fluid and orbital motion. Some of the trapped PMMA particles between biological filaments in the gaps of PS particles failed to migrate to the lower layers of the collected MPs, shown in Fig.3c, d. The different density of PMMA and PS, 1.18 g/cm^3 and 1.05 g/cm^3 , respectively, is another factor for the segregation of MPs in wastewater. The influence of density on segregation is even greater if the denser PMMA in the mixture is smaller. Both PS and PMMA samples are spherical, hence, they have the highest flowability and are easier to mix and segregate compared to non-spherical particles. In addition, adsorption of wastewater constituents on MPs surfaces can drastically change their shapes and thus segregation tendency (Pohlman et al., 2006; Abreu et al., 2003).

Fig.3c represents self-assembled biopolymers of fatty acids between the gaps of PS particles. The fatty acids in the filaments are aligned with the head to the PS particles and the tail along the length of the bridge between the MPs, which is due to the partial adsorption of the hydrophobic part of the fat molecules on the PS surfaces. The filaments formed a net-like structure (See Fig. 3c, d) with an average diameter of $5 \mu\text{m}$ and $9 \mu\text{m}$, respectively. The filaments resulted from a bi-layer assembly of fatty acid molecules in water induced by hydrophobic forces between the PS surfaces and their contrast with the hydrophilic force of the polar carboxyl group of the fat molecules. According to the Gibbs model, these molecules begin to separate from the water-soluble form via interfacial access and form a hydrophobic bilayer with heads toward the water, allowing the boundary and the length of the filament to expand (Nikpay et al., 2015). Fig.3c also shows that the filaments covered the PMMA surfaces and could not segregate with the generated mechanical vibrations in the batch. The fatty acids filaments in Fig.3d exhibit several geometric 5- or 6-sided star shapes between PS particles and were gradually rolled up and knitted.

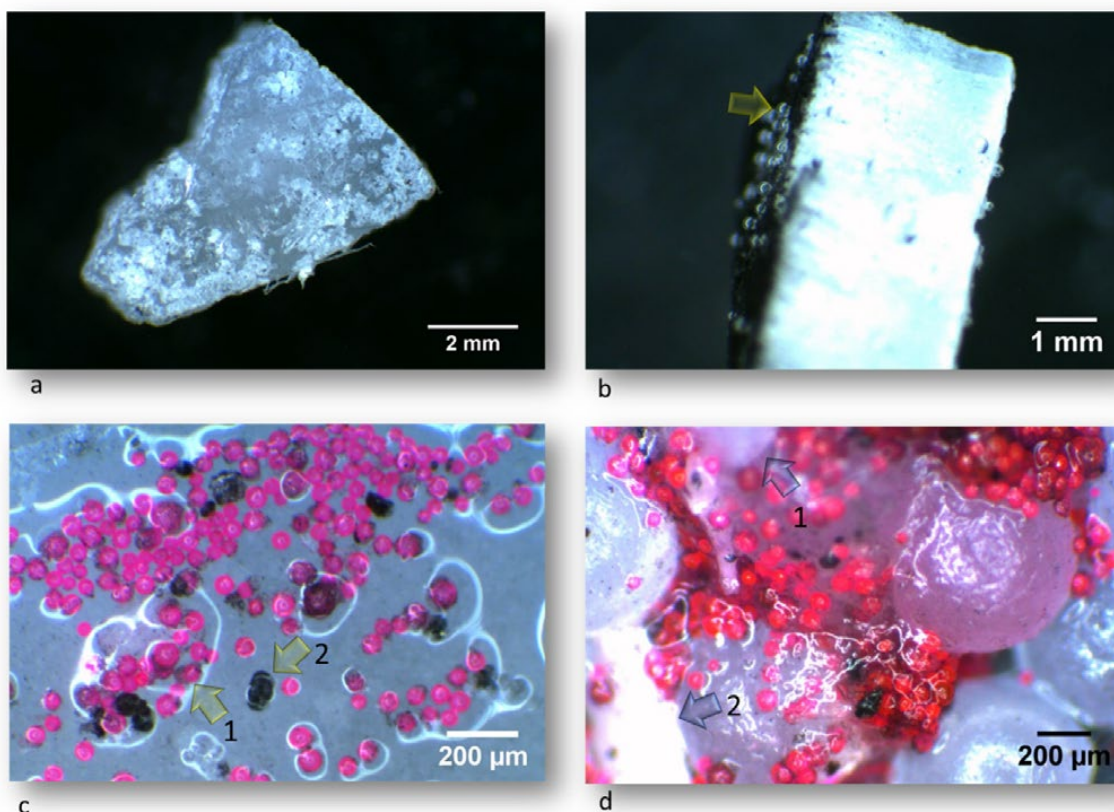


Fig. 4. The images show a) solid deposition of FOG and b) the attachment of micro-bubbles to the solid deposit surfaces. c) Adhesion of PMMA (1) and quartz (2) to the solid surfaces of deposit, d) the transformation of the gel-like phase into a solid phase (1), and a solid deposit (2).

Solid deposits

Part of the FOG deposits in bulk exhibited as white solids. Fig.4.a displays a small piece of the solid FOG deposit with a Feret diameter of 8.6 mm and a total area of 31.3 mm² produced in the batch experiment without MPs. The rigid texture of the FOG production results from the neutral pH of the liquid (Dominic et al., 2013). The small dark spots on the surface of FOG are magnetite particles (Fe₃O₄) that increase the density of the deposit. Adsorption of surfactants on Fe^{+2,3} could change the electrostatic properties of the latter, and the magnetite particles adsorb on the hydrophobic surfaces of the solid particles.

Fig.4.b shows abundant micro-bubbles attached to the FOG deposit due to its hydrophobic surfaces, inducing the deposit to be more susceptible to adsorption of pollutants. In bulk, the free surfactant molecules and macromolecules of fat can actively adsorb onto the liquid-air interfaces of the bubble, leading to its growth and making it a platform for adsorption of micro- and nano-sized plastics.

After adding MP into bulk, the red PMMA particles adhered to the FOG surfaces, as shown in Fig.4.c. The image also shows large numbers of fine quartz particles coated with dark magnetite particles adhered to the FOG surfaces.

Fig.4.d shows the occurrence of gel-like and solid FOG deposits between PS and PMMA particles. A part of the gel-like deposit from inside transformed into a white solid and formed solid/liquid phase equilibrium. The liquid phase serves as a precursor phase for the subsequent solid soap. Consequently, the separation of the liquid/liquid phase in bulk increases the

concentration of FOG materials in one of the liquid phases, e.g. in gel-like phase, allowing the fat molecules and other FOG-formative components to condense into the solid phase.

CONCLUSION

This study addressed several critical research gaps by identifying MPs directly in FOG deposits of sewer pipes and providing new studies on the FOG formation and deposition segments. Three segments of FOG deposits from the tests were identified as micro-deposits adhered or floated in the batch, gel-like deposits and solid deposits. All three FOG formations were studied using the synthetic wastewater with two types of pure MPs, polystyrene (PS) and polymethyl methacrylate (PMMA), of sizes 900 μm and 60 μm , respectively.

A strong adhesion force was found between MPs samples and three different FOG segments, which could influence the quantity and quality of sediments in the sewer system. The PS and PMMA were confined in the FOG materials and separated from the bulk, while they segregated and bond together by the self-assembled biopolymers.

The results of our study show that FOG buildup in the sewers may potentially contain large quantities of MPs, making this deposit a major hazard to the environment.

ACKNOWLEDGMENT

The author thanks the Helmholtz-Zentrum Dresden-Rossendorf (HZDR) to allow using the laboratory equipment of this institution and Neda Eghtesadi, for her assistance with the research and resources.

GRANT SUPPORT DETAILS

This work was supported by the SAB (Microplastic Separator Project, No. 716052121).

CONFLICT OF INTEREST

The author declares that there is no conflict of interests regarding the publication of this manuscript.

LIFE SCIENCE REPORTING

No life science threat was practiced in this research.

REFERENCES

- Abreu, C.R., Tavares, F.W. and Castier, M. (2003). Influence of particle shape on the packing and on the segregation of spherocylinders via Monte Carlo simulations. *Powder Technology*, 134(1-2), [https://dx.doi.org/10.1016/S0032-5910\(03\)00151-7](https://dx.doi.org/10.1016/S0032-5910(03)00151-7)
- Adib, D., Mafigholami, R. and Tabeshkia, H. (2021). Identification of microplastics in conventional drinking water treatment plants in Tehran, Iran. *Journal of Environmental Health Science and Engineering*, 19(2), <https://doi.org/10.1007/s40201-021-00737-3>
- Ainali, N.M., Kalaronis, D., Evgenidou, E., Kyzas, G.Z., Bobori, D., Kaloyianni, M., Yang, X., Bikiaris, D.N. and Lambropoulou, D.A. (2022). Do poly (lactic acid) microplastics instigate a threat? A perception for their dynamic towards environmental pollution and toxicity. *Science of the Total Environment*, <https://doi.org/10.1016/j.scitotenv.2022.155014>
- Alavian Petroody, S.S., Hashemi, S.H. and Van Gestel, C.A., (2021). No seasonal differences in the emission of microplastics from an urban wastewater treatment plant on the Southern Coast of the

- Caspian Sea, Pollution, 7(2), <https://doi.org/10.22059/poll.2021.317403.996>
- Azizi, N., Nasser, S., Nodehi, R.N., Jaafarzadeh, N. and Pirsahab, M. (2022). Evaluation of conventional wastewater treatment plants efficiency to remove microplastics in terms of abundance, size, shape, and type: A systematic review and Meta-analysis. *Marine Pollution Bulletin*, 177, <https://doi.org/10.1016/j.marpolbul.2022.113462>
- Bansagi Jr, T., Wrobel, M.M., Scott, S.K. and Taylor, A.F. (2013). Motion and Interaction of Aspirin Crystals at Aqueous–Air Interfaces. *The Journal of Physical Chemistry B*, 117(43), <https://doi.org/10.1021/jp405364c>
- Bergfreund, J., Siegenthaler, S., Lutz-Bueno, V., Bertsch, P. and Fischer, P. (2021). Surfactant Adsorption to Different Fluid Interfaces. *Langmuir*, <https://dx.doi.org/10.1021/acs.langmuir.1c00668>
- Bielefeldt, A., Gutierrez-Padilla, M.G.D., Ovtchinnikov, S., Silverstein, J. and Hernandez, M. (2010). Bacterial kinetics of sulfur oxidizing bacteria and their biodeterioration rates of concrete sewer pipe samples. *Journal of Environmental Engineering*, 136(7), [https://dx.doi.org/10.1061/\(ASCE\)EE.1943-7870.0000215](https://dx.doi.org/10.1061/(ASCE)EE.1943-7870.0000215)
- Clark, B.A. and Brown, P.W. (1999). Formation of ettringite from monosubstituted calcium sulfoaluminate hydrate and gypsum. *Journal of the American Ceramic Society*, 82(10), <https://dx.doi.org/10.1111/j.1151-2916.1999.tb02174.x>
- Dehghani, S., Moore, F. and Akhbarizadeh, R. (2017). Microplastic pollution in deposited urban dust, Tehran metropolis, Iran. *Environmental Science and Pollution Research*, 24(25), <https://doi.org/10.1007/s11356-017-9674-1>
- Dominic, C.C.S., Szakasits, M., Dean, L.O. and Ducoste, J.J. (2013). Understanding the spatial formation and accumulation of fats, oils and grease deposits in the sewer collection system. *Water science and technology*, 68(8), <https://dx.doi.org/10.2166/wst.2013.428>
- Gross, M.A., Jensen, J.L., Gracz, H.S., Dancer, J. and Keener, K.M. (2017). Evaluation of physical and chemical properties and their interactions in fat, oil, and grease (FOG) deposits. *Water research*, 123, <https://dx.doi.org/10.1016/j.watres.2017.06.072>
- He, X., Francis Iii, L., Leming, M.L., Dean, L.O., Lappi, S.E. and Ducoste, J.J. (2013). Mechanisms of fat, oil and grease (FOG) deposit formation in sewer lines. *Water research*, 47(13), <https://dx.doi.org/10.1016/j.watres.2013.05.002>
- He, X., Iasmin, M., Dean, L.O., Lappi, S.E., Ducoste, J.J. and de los Reyes III, F.L. (2011). Evidence for fat, oil, and grease (FOG) deposit formation mechanisms in sewer lines. *Environmental science & technology*, 45(10), <https://dx.doi.org/10.1021/es2001997>
- Howse, J.R., Steitz, R., Pannek, M., Simon, P., Schubert, D.W. and Findenegg, G.H. (2001). Adsorbed surfactant layers at polymer/liquid interfaces. A neutron reflectivity study. *Physical Chemistry Chemical Physics*, 3(18), pp.4044-4051
- Huber, B., Herzog, B., Drewes, J.E., Koch, K. and Müller, E. (2016). Characterization of sulfur oxidizing bacteria related to biogenic sulfuric acid corrosion in sludge digesters. *BMC microbiology*, 16(1), <https://dx.doi.org/10.1186/s12866-016-0767-7>
- Ida, S. and Eva, T. (2021). Removal of Heavy Metals during Primary Treatment of Municipal Wastewater and Possibilities of Enhanced Removal: A Review. *Water*, 13(8), <https://doi.org/10.3390/w13081121>
- Igathinathane, C., Pordesimo, L.O., Columbus, E.P., Batchelor, W.D. and Methuku, S.R. (2008). Shape identification and particles size distribution from basic shape parameters using ImageJ. *Computers and electronics in agriculture*, 63(2).
- Ingram, T., Storm, S., Kloss, L., Mehling, T., Jakobtorweihen, S. and Smirnova, I. (2013). Prediction of micelle/water and liposome/water partition coefficients based on molecular dynamics simulations, COSMO-RS, and COSMOmic. *Langmuir*, 29(11), <https://dx.doi.org/10.1021/la305035b>
- Jain, A., Metzger, M.J. and Glasser, B.J. (2013). Effect of particle size distribution on segregation in vibrated systems. *Powder technology*, 237, <https://dx.doi.org/10.1016/j.powtec.2012.12.044>
- Keener, K.M., Ducoste, J.J. and Holt, L.M. (2008). Properties influencing fat, oil, and grease deposit formation. *Water environment research*, 80(12), <https://dx.doi.org/10.2175/193864708X267441>
- Li, X., Kappler, U., Jiang, G. and Bond, P.L. (2017). The ecology of acidophilic microorganisms in the corroding concrete sewer environment. *Frontiers in microbiology*, 8, <https://dx.doi.org/10.3389/fmicb.2017.00683>
- Li, Y., Pham, J.Q., Johnston, K.P. and Green, P.F. (2007). Contact angle of water on polystyrene thin films: Effects of CO₂ environment and film thickness. *Langmuir*, 23(19), <https://dx.doi.org/10.1021/la0636311>

- Nieuwenhuis, E., Langeveld, J. and Clemens, F. (2018). The relationship between fat, oil and grease (FOG) deposits in building drainage systems and FOG disposal patterns. *Water Science and Technology*, 77(10), <https://dx.doi.org/10.2166/wst.2018.173>
- Nikpay, M. (2022). Wastewater Fines Influence the Adsorption Behavior of Pollutants onto Microplastics. *Journal of Polymers and the Environment*, 30(2), <https://doi.org/10.1007/s10924-021-02243-x>
- Nikpay, M., Lazik, D. and Krebs, P. (2015). Water displacement by surfactant solution: an experimental study to represent wastewater loss from sewers to saturated soil. *International journal of environmental science and technology*, 12(8), <https://dx.doi.org/10.1007/s13762-014-0681-1>
- O'Connell, M., McNally, C. and Richardson, M.G. (2010). Biochemical attack on concrete in wastewater applications: A state of the art review. *Cement and Concrete Composites*, 32(7), <https://dx.doi.org/10.1016/j.cemconcomp.2010.05.001>
- Otsuka, T., Yamazaki, H., Ankyu, E., Ahamed, T., Anda, M. and Noguchi, R. (2020). Elucidation of the mechanism of blockage in sewer pipes by fatty acid deposition and suspended solid. *Water*, 12(8), <https://dx.doi.org/10.3390/w12082291>
- Pohlman, N.A., Severson, B.L., Ottino, J.M. and Lueptow, R.M. (2006). Surface roughness effects in granular matter: Influence on angle of repose and the absence of segregation. *Physical Review E*, 73(3), <https://dx.doi.org/10.1103/PhysRevE.73.031304>
- Razeghi, N., Hamidian, A.H., Wu, C., Zhang, Y. and Yang, M. (2021). Scientific studies on microplastics pollution in Iran: an in-depth review of the published articles. *Marine Pollution Bulletin*, 162, <https://doi.org/10.1016/j.marpolbul.2020.111901>
- Roberts, D.J., Nica, D., Zuo, G. and Davis, J.L. (2002). Quantifying microbially induced deterioration of concrete: initial studies. *International Biodeterioration & Biodegradation*, 49(4), pp.227-234, [https://doi.org/10.1016/S0964-8305\(02\)00049-5](https://doi.org/10.1016/S0964-8305(02)00049-5)
- Satoh, H., Odagiri, M., Ito, T. and Okabe, S. (2009). Microbial community structures and in situ sulfate-reducing and sulfur-oxidizing activities in biofilms developed on mortar specimens in a corroded sewer system. *Water research*, 43(18), <https://dx.doi.org/10.1016/j.watres.2009.07.035>
- Schessl, M., Johns, C. and Ashpole, S.L. (2019). Microbeads in Sediment, Dreissenid Mussels, and Anurans in the Littoral Zone of the Upper St. Lawrence River, New York. *Pollution*, 5(1), <https://doi.org/10.22059/poll.2018.257596.468>
- Sepehr, M.N., Zarrabi, M., Kazemian, H., Amrane, A., Yaghmaian, K. and Ghaffari, H.R. (2013). Removal of hardness agents, calcium and magnesium, by natural and alkaline modified pumice stones in single and binary systems. *Applied Surface Science*, 274, <https://dx.doi.org/10.1016/j.apsusc.2013.03.042>
- Tokuda, K., Ogino, T., Kotera, M. and Nishino, T. (2015). Simple method for lowering poly (methyl methacrylate) surface energy with fluorination. *Polymer Journal*, <https://dx.doi.org/10.1038/pj.2014.91>
- Verdú, I., Amariei, G., Plaza-Bolaños, P., Agüera, A., Leganés, F., Rosal, R. and Fernández-Piñas, F. (2022). Polystyrene nanoplastics and wastewater displayed antagonistic toxic effects due to the sorption of wastewater micropollutants. *Science of the Total Environment*, <https://doi.org/10.1016/j.scitotenv.2022.153063>.
- Viaroli, S., Lancia, M. and Re, V. (2022). Microplastics contamination of groundwater: Current evidence and future perspectives. A review. *Science of the Total Environment*, <https://doi.org/10.1016/j.scitotenv.2022.153851>
- Wallace, T., Gibbons, D., O'Dwyer, M. and Curran, T.P. (2017). International evolution of fat, oil and grease (FOG) waste management—A review. *Journal of environmental management*, 187, <https://dx.doi.org/10.1016/j.jenvman.2016.11.003>
- Williams, J.B., Clarkson, C., Mant, C., Drinkwater, A. and May, E. (2012). Fat, oil and grease deposits in sewers: Characterisation of deposits and formation mechanisms. *Water research*, 46(19), <https://dx.doi.org/10.1016/j.watres.2012.09.002>

